Chinese Chemical Letters 31 (2020) 2512–2515

Contents lists available at ScienceDirect

Chinese Chemical Letters

journal homepage: www.elsevier.com/locate/cclet

Communication

Highly dispersed Ru/Co catalyst with enhanced activity for catalyzing $NaBH_4$ hydrolysis in alkaline solutions

Jiapeng Zhang, Fanzhen Lin, Lijing Yang, Hua Dong*

College of Materials and Chemistry & Chemical Engineering, Chengdu University of Technology, Chengdu 610059, China

ARTICLE INFO

Article history:
Received 5 February 2020
Received in revised form 16 March 2020
Accepted 28 March 2020
Available online 13 April 2020

Keywords:
Ru/Co
$NaBH_4$
Catalytic hydrolysis
Hydrogen generation
Heterogeneous catalysis

ABSTRACT

Ru and Co are highly dispersed on the surface of TiO_2 nanoparticles with an easy coprecipitation method to fabricate a novel Ru-based catalyst (Ru/Co-TiO_2). The fabricated Ru/Co-TiO_2 catalyst exhibits superior catalytic performance for promoting $NaBH_4$ hydrolysis in alkaline medium, showing an impressive hydrogen generation rate per gram Ru as high as 172 L min^{-1} g_{Ru}^{-1}, which is better than most of recently reported Ru-based catalysts. In addition, the fabricated Ru/Co-TiO_2 catalyst also shows excellent durability in cycle use, with only 2.9% activity loss after being used for 5 cycles. These advantages make the developed Ru/Co-TiO_2 catalyst a potential choice for promoting hydrogen generation from $NaBH_4$ hydrolysis.

Due to the distinct advantages including stability, high hydrogen storage capacity, hydrolysis controllability and high hydrogen purity, borohydrides form a kind of very promising hydrogen storage materials [1–5]. A typical representative of them is sodium borohydride ($NaBH_4$) [6,7]. The hydrolysis of 1 g $NaBH_4$ can release 0.21 g hydrogen with high purity. However, the self-hydrolysis of $NaBH_4$ without a catalyst is extremely slow [7,8]. Therefore, great efforts have been made to develop suitable catalysts which could endow $NaBH_4$ hydrolysis decent rates [9–11].

Varieties of metal catalysts, such as Ru [12–19], Pd [13,20], Co [21–32], Ni [32–36] and complexes of them [37–46], were extensively studied in the last years. Plenty of researches suggest that Ru-based catalysts have excellent activity in catalyzing $NaBH_4$ hydrolysis [8,12–15,40,41]. Nevertheless, although monometallic Ru catalysts have high activity for catalyzing $NaBH_4$ hydrolysis under neutral conditions, their performance is dramatically compromised under alkaline conditions [19,38]. Yet, $NaBH_4$ solutions are usually stabilized in alkaline environment to prevent the uncontrolled self-hydrolysis. On the contrary, when Ru iscombined with other metals, the formed complex catalysts could maintain the high catalytic activity for $NaBH_4$ hydrolysis under alkaline conditions [15,41]. Furthermore, considering the high cost and scarcity of Ru metal, it is very important to develop catalysts with special composition and nano/microstructures to improve the Ru efficiency. For this propose, Ru species in the catalysts must be dispersed well enough. It means that the catalysts composed of Ru nanoparticles, clusters, or even single atoms are highly demanded. However, free Ru nanoparticles, clusters, or single atoms are not stable. They tend to aggregate to reduce the surface energy. Thus, varieties of substrates have been employed to support Ru species to improve their stability [12–15,40–43]. Nevertheless, Ru species in these catalysts is normally in the form of nanoparticles, leaving space for further reducing the size to improve the catalytic efficiency.

Herein, we report a novel Ru-based catalyst (Ru/Co-TiO_2), which was fabricated through coprecipitation of Ru^{3+} and Co^{2+} on TiO_2 nanoparticles in aqua regia. Ru and Co species in this catalyst were well dispersed. $NaBH_4$ hydrolysis experiments in alkaline solutions showed that the Ru/Co-TiO_2 catalyst had superior catalytic activity and durability.

Scheme 1 shows an illustration of the fabrication of the Ru/Co-TiO_2 catalyst. Briefly, $RuCl_3{\cdot}3H_2O$ and $Co(NO_3)_2{\cdot}6H_2O$ were firstly dissolved in aqua regia to form a homogenous solution, into which TiO_2 nanoparticles (~40 nm) were added. The mixture was stirred in 140 °C oil bath until it was dry. The obtained solid was then reduced in aqueous solution of ammonia borane, washed with water and dried at 60 °C in vacuum overnight to obtain Ru/Co-TiO_2 catalyst. Ru-TiO_2 and Co-TiO_2 were fabricated for control experiments with the same method, but without $Co(NO_3)_2{\cdot}6H_2O$ or $RuCl_3{\cdot}3H_2O$ in the original aqua regia solutions, respectively.

After the successful fabrication, the loading density of Ru and Co in the catalysts was measured with inductively coupled plasma-optical emission spectroscopy (ICP-OES). The results demonstrated that Ru/Co-TiO_2 catalyst had 0.06 wt% Ru and 0.61 wt% Co, while

* Corresponding author.
E-mail address: donghua@iccas.ac.cn (H. Dong).

https://doi.org/10.1016/j.cclet.2020.03.072
1001-8417/

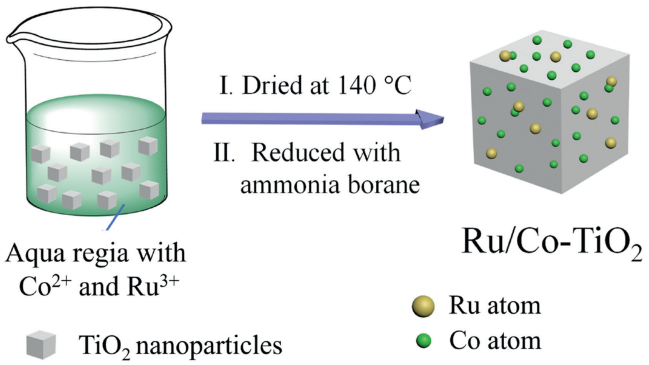

Scheme 1. Schematic illustration of the fabrication of Ru/Co-TiO_2.

Ru-TiO_2 and Co-TiO_2 had 0.09 wt% Ru and 0.77 wt% Co, respectively. The Brunauer-Emmett-Teller (BET) surface measurement indicated that TiO_2 nanoparticles used as the substrate had a specific surface area of 64.3 m^2/g. Considering the low density of Ru and Co, the high surface area of TiO_2 could provide sufficient space for them to anchor.

Transmission electron microscopy (TEM) and high-angle annular dark field-scanning transmission electron microscopy (HAADF-STEM) images in Fig. 1 have shown the structures of the fabricated Ru/Co-TiO_2 catalyst. The lattice fringes highlighted in Fig. 1b show the planes with interplanar spacing of 3.5 Å, corresponding to the (101) planes of TiO_2. However, due to their far lower density than Ti, no distinct Co and Ru atoms could be observed with HAADF-STEM, which is consistent with the results previously reported by Tao *et al.* [47]. This also verified the good distribution of Co and Ru species in the sample. As Co and Ru species could not be observed directly from HAADF-STEM images, elemental mapping was carried out to verify their existence (Fig. 1c). It could be clearly seen that the Co and Ru species sparsely dispersed on TiO_2 nanoparticles, and that the signal of Co was distinctly stronger than Ru, which was consistent with their different loading density.

To further analyze the surface of the Ru/Co-TiO_2 catalyst, X-Ray Photoelectron Spectroscopy (XPS) investigations were carried out. Fig. S1a (Supporting information) shows the full survey XPS spectrum of the Ru/Co-TiO_2 catalyst. In the spectrum the peaks of Ti and O could be unambiguously observed, while the peaks of Ru and Co were not significantly visible. Due to the low content of Ru and the disturbance of Ti 2p peaks, the Ru 3p peaks could not be distinguished during fine scanning (Fig. S1b in Supporting information). Nevertheless, the Co 2p peaks in Fig. S1c (Supporting information) distinctly show that Co species in the catalyst had two oxidation states. The peaks at 786.0 eV and 801.7 eV corresponded to Co^{2+}, and the peaks at 780.9 eV and 796.4 eV corresponded to Co^{3+}. The analysis based on XPS investigation has further confirmed the low content of Ru and Co species in the Ru/Co-TiO_2 catalyst. In addition, the X-ray Diffraction (XRD) pattern in Fig. S2 (Supporting information) shows apparent diffraction peaks of Ru/Co-TiO_2 catalyst, while all of them belong to the planes of TiO_2. No diffraction peaks associated to Ru or Co species could be observed, indicating the lack of related nanoparticles again.

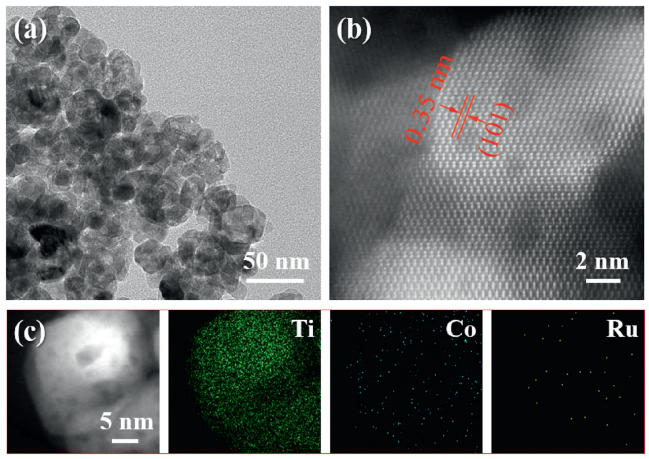

Fig. 1. (a) TEM image of Ru/Co-TiO_2. (b) HAADF-STEM image of Ru/Co-TiO_2. Interplanar spacing of 0.35 nm corresponds to (101) planes of TiO_2. No Co or Ru nanoparticles could be observed. (c) Elemental mapping of Ti, Co and Ru in the Ru/Co-TiO_2 catalyst. Co and Ru could be observed sparsely dispersed on the surface of TiO_2 nanoparticles.

The catalytic performance of the fabricated Ru/Co-TiO_2 catalyst was evaluated with catalyzed $NaBH_4$ hydrolysis under different conditions in a home-built setup [48]. In a typical experiment, 100 mg catalyst and 25 mg $NaBH_4$ were mixed in an aqueous medium with 10 wt% NaOH to form 10 g reaction mixture to start the catalyzed hydrolysis, and the $NaBH_4$ hydrolysis rate was reflected by the hydrogen generation (HG) rate. Various factors which influenced the hydrolysis rate including composition of catalysts, NaOH concentration, $NaBH_4$ concentration, catalyst dosage and temperature were investigated in detail.

Aqueous solutions of $NaBH_4$ are usually stabilized under alkaline conditions to prevent the unwanted self-hydrolysis. Therefore, a competent catalyst should have high activity for catalyzing $NaBH_4$ hydrolysis under alkaline conditions. In our study, we performed $NaBH_4$ hydrolysis experiments with different NaOH concentrations from 0 to 20 wt% (Fig. 2). It was found that $NaBH_4$ hydrolysis catalyzed by Ru/Co-TiO_2 had the highest HG rate of 10.34 mL/min when NaOH concentration was 10 wt%. Considering the loading density of Ru in the catalyst (0.06 wt%), the HG rate per gram Ru could be calculated to be 172 L min^{-1} g_{Ru}^{-1}. This value is higher than the Ru efficiency of most recently reported Ru-based catalysts (Table S1 in Supporting information) [13–18,39–41]. If the average HG rate was calculated based on the amount of Co in the catalyst, it was 17 L min^{-1} g_{Co}^{-1}, also very high due to the contribution of Ru (Table S2 in Supporting information) [23–27].

When NaOH concentration was lower than 10 wt%, the existence of NaOH apparently accelerated the catalyzed $NaBH_4$ hydrolysis. However, when the concentration of NaOH was too high (higher than 10 wt%), the hydrolysis reaction became slower. It is widely accepted that the slowdown of the hydrolysis reaction when NaOH concentration was too high was caused by the increasing viscosity of the reaction mixture, but how low concentration of NaOH accelerated the catalyzed $NaBH_4$ hydrolysis is still unknown.

The Co-TiO_2 catalyst showed a similar trend as Ru/Co-TiO_2, providing highest catalytic activity when NaOH concentration was 12.5 wt%. This is consistent with the results reported in previous studies [30,32,46]. However, Ru-TiO_2 showed a different trend. The HG rate of the reactions catalyzed by Ru-TiO_2 (3.65 mL/min) was on the same level with Ru/Co-TiO_2 (5.47 mL/min) when NaOH was absent. But the existence of NaOH had distinct inhibiting effect for Ru-TiO_2 catalyst. With the increasing of NaOH concentration, the $NaBH_4$ hydrolysis rate decreased dramatically. When NaOH concentration was above 12.5 wt%, hydrogen could hardly be produced.

To elucidate the impact of $NaBH_4$ concentration on the rate of hydrolysis catalyzed by Ru/Co-TiO_2, experiments with different $NaBH_4$ concentrations were carried out. It could be concluded from Figs. 3a and b that the hydrolysis rate increased sharply when $NaBH_4$ concentration was increased from 0.10 wt% to 0.25 wt%, but deceased gradually when $NaBH_4$ concentration was further increased from 0.25 wt% to 10 wt%. As shown in Fig. 3a, when $NaBH_4$ concentration was higher than 0.25 wt%, hydrogen bubbles

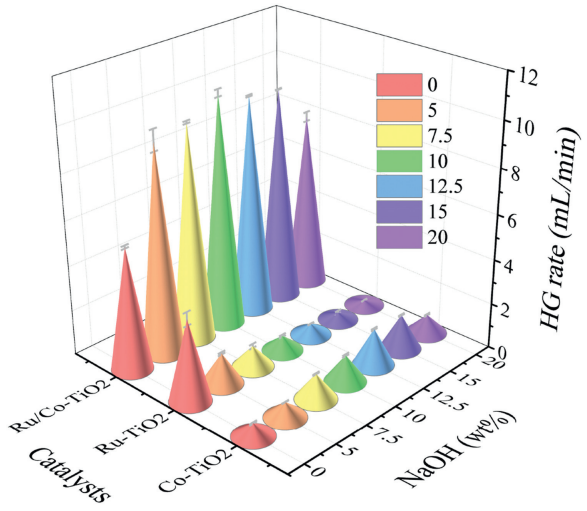

Fig. 2. The HG rates of $NaBH_4$ hydrolysis catalyzed by Ru/Co-TiO_2, Ru-TiO_2, or Co-TiO_2 under different NaOH concentrations. Experimental conditions: 100 mg catalysts, 25 mg $NaBH_4$, 30 °C.

emerged as soon as the $NaBH_4$ solution was mixed with Ru/Co-TiO_2 catalyst. However, if $NaBH_4$ concentration decreased from 0.25 wt%, the initiation of the hydrolysis reaction gradually became more difficult, and therefore the volume of hydrogen generated at the very beginning was very little. Actually, in the catalyzed $NaBH_4$ hydrolysis experiments, we noticed that the colour of the Ru/Co-TiO_2 catalyst changed from grey to black during the reactions. When $NaBH_4$ concentration was low enough, it could be further observed that hydrogen bubbles could be generated in the solution only after the colour change of the catalyst had finished. This was

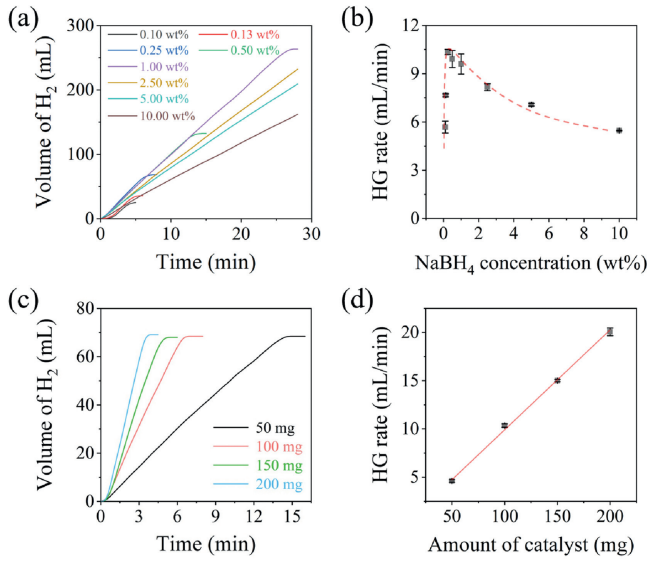

Fig. 3. (a, b) $NaBH_4$ hydrolysis under conditions with different $NaBH_4$ concentrations. (a) Plots of H_2 volume *versus* time for hydrolysis reactions with different $NaBH_4$ concentrations. (b) The HG rates of hydrolysis reactions with different $NaBH_4$ concentrations; Experimental conditions: 10 wt% NaOH, 100 mg Ru/Co-TiO_2, 30 °C. (c, d) $NaBH_4$ hydrolysis under conditions with different Ru/Co-TiO_2 dosages. (c) Plots of H_2 volume *versus* time for hydrolysis reactions catalyzed by different amount of Ru/Co-TiO_2. (d) The HG rates of hydrolysis reactions catalyzed by different amount of Ru/Co-TiO_2; Experimental conditions: 10 wt% NaOH, 25 mg $NaBH_4$, 30 °C.

consistent with the phenomenon reported by Demirci *et al.* in 2011 [49]. It indicates that the active form of the catalyst might not be the fresh prepared Ru/Co-TiO_2, but be some product from Ru/Co-TiO_2 reacted with $NaBH_4$ solution. This is a very important point for the investigation on the potential mechanisms of $NaBH_4$ hydrolysis catalyzed by Ru/Co-TiO_2. However, as emphasized by Demirci *et al.*, the elucidation of the mechanisms will be a much tougher work to do [50]. Anyway, due to the lag phase at the beginning, the average hydrolysis rate of reactions decreased sharply as $NaBH_4$ concentration decreased from 0.25 wt% (Fig. 3b). However, when $NaBH_4$ concentration was increased from 0.25 wt%, the difference at the very beginning of the reactions became not distinguishable. On the contrary, with the increase of $NaBH_4$ concentration, the increase of solution viscosity and the formation of more $NaBO_2$ around the catalyst nanoparticles started to hinder mass exchange in the reaction [33,43,46]. As a result, the general hydrolysis rate gradually decreased (Fig. 3b). Nevertheless, although the increase of $NaBH_4$ concentration brought about acceleration or slowdown of hydrolysis reactions, the yield of hydrogen was not significantly affected. The final volume of hydrogen generated increased proportionally with the increasing of $NaBH_4$ concentration (Fig. S3 in Supporting information).

The change of dosage of the Ru/Co-TiO_2 catalyst dramatically affected $NaBH_4$ hydrolysis rate in another way. As shown in Figs. 3c and d, when the catalyst amount increased from 50 mg to 200 mg, the hydrolysis rate increased linearly from 4.60 mL/min to 20.06 mL/min, indicating that the catalyst was fully utilized in the hydrolysis reactions.

Temperature plays an important role in the $NaBH_4$ hydrolysis as it is an exothermic reaction. To investigate the temperature effects on our system, the reactions were carried out at 30 °C, 40 °C, 50 °C and 60 °C. As shown in Figs. 4a and b, the $NaBH_4$ hydrolysis rate increased sharply with the increasing of temperature. The HG rate of the hydrolysis reactions at 30 °C was just 10.34 mL/min, while it jumped to 45.54 mL/min when it was 60 °C, with 3.4 times increasing (Fig. 4b). Moreover, the activation energy (E_a) of the hydrolysis reactions catalyzed by Ru/Co-TiO_2 was calculated with Arrhenius equation (Eq. 1):

$$\ln k = \ln A - E_a/RT \quad (1)$$

Where T is the reaction temperature of $NaBH_4$ hydrolysis in Kelvin (K), k is the rate constant of the hydrolysis reaction, R is the gas constant, and A is pre-exponential factor. Based on the $NaBH_4$ hydrolysis rates reflected by the HG rates at different temperatures, the E_a was calculated to be 38.74 kJ/mol (Fig. 4c), which is comparable with the E_a of $NaBH_4$ hydrolysis reactions catalyzed by other reported Ru-based catalysts (Table S1 in Supporting information) [13–17,39–41], demonstrating good catalytic activity of Ru/Co-TiO_2.

To verify the practicability of Ru/Co-TiO_2 in practical applications, the durability tests were carried out by evaluating the activity of catalyst in cycle use. After each use, the used catalyst was collected from the reaction mixture by centrifuging, washed with water, and dried in vacuum at 60 °C. And then it was used for catalyzing $NaBH_4$ hydrolysis again. As show in Fig. 4d, the $NaBH_4$ hydrolysis rate at the 55th cycle was 97.1% of the rate at 1st cycle. After the 5th experiment, the used catalyst was further characterized with high resolution TEM, XPS and XRD. The results (Fig. S4 in Supporting information) showed that no significant changes could be observed on the catalyst after being used for 5 cycles. It demonstrates that the Ru/Co-TiO_2 catalyst had excellent durability in catalyzing $NaBH_4$ hydrolysis.

In summary, a Ru/Co-TiO_2 catalyst composed of TiO_2 nanoparticles with Ru and Co species highly dispersed on the surface was developed by coprecipitation of Ru^{3+} and Co^{2+} on TiO_2 nanoparticles in aqua regia. The structures and chemical

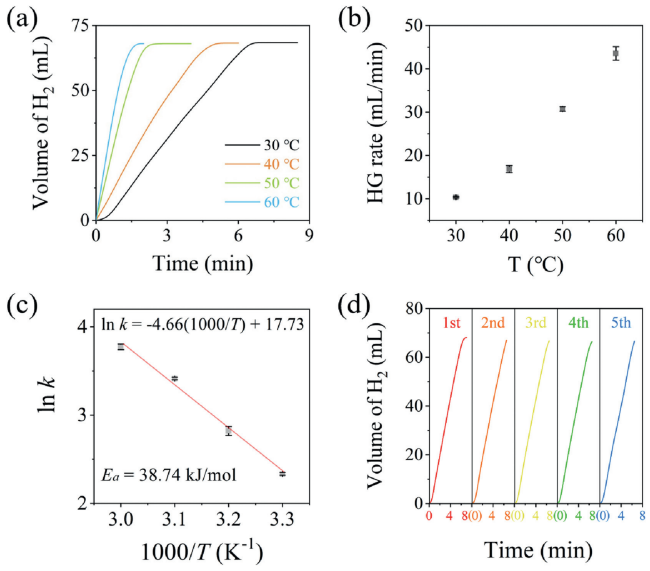

Fig. 4. (a-c) The impact of temperature on Ru/Co-TiO_2 catalyzed $NaBH_4$ hydrolysis. (a) Plots of H_2 volume *versus* time for hydrolysis reactions at different temperatures. (b) The HG rates of hydrolysis reactions catalyzed by Ru/Co-TiO_2 at different temperatures. (c) Arrhenius plot for Ru/Co-TiO_2 catalyzed $NaBH_4$ hydrolysis; Experiment conditions: 10 wt% NaOH, 25 mg $NaBH_4$, 100 mg Ru/Co-TiO_2. (d) The durability of Ru/Co-TiO_2 in multi-cyclic $NaBH_4$ hydrolysis. Experimental conditions: 10 wt% NaOH, 25 mg $NaBH_4$, 100 mg Ru/Co-TiO_2, 30 °C.

compositions of the Ru/Co-TiO_2 catalyst were verified with ICP-OES, TEM, HAADF-STEM, XPS, and XRD investigations. The experimental results showed that the Ru/Co-TiO_2 catalyst had superior performance for catalyzing $NaBH_4$ hydrolysis in the alkaline solution with 10 wt% NaOH, providing a hydrogen generation rate per gram Ru at 30 °C as high as 172 L min^{-1} g_{Ru}^{-1}, better than most of the previously reported Ru-based catalysts. Moreover, the Ru/Co-TiO_2 catalyst also showed excellent durability in cycle use, with just 2.9% of activity loss after being used for 5 times. These advantages made it a potential choice for catalyzing $NaBH_4$ hydrolysis to supply hydrogen in portable systems.

Declaration of competing interest

The authors declare that they have no known competing financial interests or personal relationships that could have appeared to influence the work reported in this paper.

Appendix A. Supplementary data

Supplementary material related to this article can be found, in the online version, at doi:https://doi.org/10.1016/j.cclet.2020.03.072.

References

[1] U.B. Demirci, P. Miele, Energy Environ. Sci. 2 (2009) 627–637.
[2] C.L. Wang, J. Tuninetti, Z. Wang, et al., J. Am. Chem. Soc. 139 (2017) 11610–11615.
[3] L.B. Wang, H.L. Li, W.B. Zhang, et al., Angew. Chem. Int. Ed. 56 (2017) 4712–4718.
[4] Y.N. Men, J. Su, C.Z. Huang, et al., Chin. Chem. Lett. 29 (2018) 1671–1674.
[5] L. Wen, Z. Zheng, W. Luo, P. Cai, G.Z. Cheng, Chin. Chem. Lett. 26 (2015) 1345–1350.
[6] L.Z. Ouyang, W. Chen, J.W. Liu, et al., Adv. Energy Mater. 7 (2017) 1700299.
[7] H.I. Schlesinger, H.C. Brown, A.E. Finholt, et al., J. Am. Chem. Soc. 75 (1953) 215–219.
[8] H.C. Brown, C.A. Brown, J. Am. Chem. Soc. 84 (1962) 1493–1494.
[9] P. Brack, S.E. Dann, K.G.U. Wijayantha, Energy Sci. Eng. 3 (2015) 174–188.
[10] H.M. Sun, J. Meng, L.F. Jiao, F.Y. Cheng, J. Chen, Inorg. Chem. Front. 5 (2018) 760–772.
[11] N. Sahiner, Prog. Polym. Sci. 38 (2013) 1329–1356.
[12] J. Zhang, J.H. Hao, Q.L. Ma, et al., J. Nanopart. Res. 19 (2017) 227.
[13] G. Bozkurt, A. Ozer, A.B. Yurtcan, Energy 180 (2019) 702–713.
[14] M.H. Tan, Y. Wang, A. Taguchi, et al., Int. J. Hydrogen Energy 44 (2019) 7320–7325.
[15] D.D. Tuan, K.Y.A. Lin, Chem. Eng. J. 351 (2018) 48–55.
[16] Y. Liang, H.B. Dai, L.P. Ma, P. Wang, H.M. Cheng, Int. J. Hydrogen Energy 35 (2010) 3023–3028.
[17] J.P. Zhang, F.Z. Lin, L.J. Yang, et al., Chin. Chem. Lett. 31 (2020) 2019–2022.
[18] Y.H. Huang, C.C. Su, S.L. Wang, M.C. Lu, Energy 46 (2012) 242–247.
[19] Y.C. Zou, M. Nie, Y.M. Huang, J.Q. Wang, H.L. Liu, Int. J. Hydrogen Energy 36 (2011) 12343–12351.
[20] Y.L. Guo, J. Qian, A. Iqbal, et al., Int. J. Hydrogen Energy 42 (2017) 15167–15177.
[21] L.M. Shi, W. Xie, Z.Y. Jian, X.M. Liao, Y.J. Wang, Int. J. Hydrogen Energy 44 (2019) 17954–17962.
[22] A.F. Baye, M.W. Abebe, R. Appiah-Ntiamoah, H. Kim, J. Colloid. Interf. Sci. 543 (2019) 273–284.
[23] L.M. Shi, Z. Chen, Z.Y. Jian, F.H. Guo, C.L. Gao, Int. J. Hydrogen Energy 44 (2019) 19868–19877.
[24] C. Luo, F.Y. Fu, X.J. Yang, et al., ChemCatChem 11 (2019) 1643–1649.
[25] H.M. Zhang, X.L. Feng, L.N. Cheng, et al., Colloid Surf. A 563 (2019) 112–119.
[26] T.T. Liu, K.Y. Wang, G. Du, A.M. Asiri, X.P. Sun, J. Mater. Chem. A 4 (2016) 13053–13057.
[27] D.G. Xu, X.Y. Zhang, X. Zhao, et al., Int. J. Energy Res. 43 (2019) 3702–3710.
[28] M.H. Lee, J.R. Deka, C.J. Cheng, et al., Appl. Surf. Sci. 470 (2019) 764–772.
[29] X.Y. Zhang, X.W. Sun, D.Y. Xu, et al., Appl. Surf. Sci. 469 (2019) 764–769.
[30] N. Patel, A. Miotello, Int. J. Hydrogen Energy 40 (2015) 1429–1464.
[31] R. Edla, S. Gupta, N. Patel, et al., Appl. Catal. A -Gen. 515 (2016) 1–9.
[32] G. Bozkurt, A. Ozer, A.B. Yurtcan, Int. J. Hydrogen Energy 43 (2018) 22205–22214.
[33] J. Lee, H. Shin, K.S. Choi, et al., Int. J. Hydrogen Energy 44 (2019) 2943–2950.
[34] H.K. Cai, L.P. Liu, Q. Chen, P. Lu, J. Dong, Energy 99 (2016) 129–135.
[35] D. Kilinc, O. Sahin, Int. J. Hydrogen Energy 43 (2018) 10717–10727.
[36] Y. Wang, Y.S. Lu, D. Wang, et al., Int. J. Hydrogen Energy 41 (2016) 16077–16086.
[37] S.A. Al-Thabaiti, Z. Khan, M.A. Malik, Int. J. Hydrogen Energy 44 (2019) 16452–16466.
[38] N.X. Kang, R. Djeda, Q. Wang, et al., ChemCatChem 11 (2019) 2341–2349.
[39] M. Wen, Y.Z. Sun, X.M. Li, et al., J. Power Sources 243 (2013) 299–305.
[40] Y.S. Wei, Y. Wang, L. Wei, et al., Int. J. Hydrogen Energy 43 (2018) 592–600.
[41] J.Y. Guo, C.B. Wu, J.F. Zhang, et al., J. Mater. Chem. A 7 (2019) 8865–8872.
[42] F.H. Wang, Y.M. Luo, Y.A. Wang, H. Zhu, Int. J. Hydrogen Energy 44 (2019) 13185–13194.
[43] A.M. Pornea, M.W. Abebe, H. Kim, Chem. Phys. 516 (2019) 152–159.
[44] G. Ro, D.K. Hwang, Y. Kim, J. Ind, Eng. Chem. 79 (2019) 364–369.
[45] W.Y. Liu, H.K. Cai, P. Lu, et al., Int. J. Hydrogen Energy 38 (2013) 9206–9216.
[46] A. Didehban, M. Zabihi, J.R. Shahrouzi, Int. J. Hydrogen Energy 43 (2018) 20645–20660.
[47] X.Y. Zhang, Z.C. Sun, B. Wang, et al., J. Am. Chem. Soc. 140 (2018) 954–962.
[48] L.J. Yang, X.S. Huang, J.P. Zhang, H. Dong, ChemPlusChem 86 (2020) 399–404.
[49] O. Akdim, U.B. Demirci, P. Miele, Int. J. Hydrogen Energy 36 (2011) 13669–13675.
[50] U.B. Demirci, P. Miele, Cr. Chim. 17 (2014) 707–716.